

Miniaturized Chemical Multiplexed Sensor Array

Ming Su, Shuyou Li, and Vinayak P. Dravid*

Department of Materials Science and Engineering and Institute for Nanotechnology, Northwestern University, Evanston, Illinois 60208

Received April 21, 2003; E-mail: v-dravid@northwestern.edu

The on-site and real-time detection of hazardous gas calls for integrated sensors with low energy consumption, fast response, and rapid recovery. In some cases the sensor should be able to recognize the type of gas that induces the response. The advent of nanostructured materials with enhanced properties, and the means to pattern such materials at the nanoscale, have paved the way for improved chemical detection. Thus, the fabrication of miniaturized sensors using novel nanomaterials has recently been an active topic.

Thin films assembled from nanoparticles and nanoporous materials have been used as sensor elements for many years. The resistance change of the film upon exposure to certain gases is often the basis for the sensing action.¹ However, the size of such sensors is often quite large, and further miniaturization is difficult. The fabrication techniques, such as physical deposition, make it hard to create sensor arrays with different compositions for each sensor. One-dimensional nanowires (e.g., carbon nanotubes, silicon nanowires, and semiconductor nanoribbons) have also been used as novel sensor materials.² Proof-of-concept performance schemes have been documented. However, the necessity of separate steps in nanowires synthesis and subsequent purification and sensor fabrication requires additional parallel operations to incorporate them into microelectronics circuitry.³ For integrated multisensor fabrication, it is a challenge for parallel methods (microfluidics or random deposition from suspension) to create sensor arrays with multiple detection capability using different sensor elements.⁴

Dip-pen nanolithography (DPN) is based on the controlled transfer of molecular ink from an ink-coated tip of an atomic force microscope (AFM) to a substrate.⁵ Two unique features of DPN are its highly localized patterning capability and the serial nature of its operation, which enable successive patterning of different inks on specific locations. We have shown the patterning of metal oxide nanostructures on insulating and conducting surfaces by DPN using sol ink.⁶ The versatile sol-gel process provides many choices for suitable inks with inexpensive precursors amenable to handling in liquid form, and opens many possibilities to prepare functional structures, including sensors, catalysts, supports, etc.⁷

Herein, we describe an efficient approach for the construction of miniaturized semiconductor chemical sensors by exploiting the capabilities of DPN in site-specific and multiple ink patterning, and the versatility of sol-gel synthesis to prepare appropriate sol inks. The method allows the construction of fast-response and rapid-recovery sensors and a combinatorial array in the search for good sensor materials. It also paves the way for an on-chip electronic sensor array, capable of discriminating various gaseous species with collective reference responses from all the sensor elements.

An improved ink coating and patterning method has been developed, which combines the operation of micro-pen patterning and DPN, thus providing more control and flexibility over previous methods. Briefly, 5- μ L droplets of sol inks are deposited on a substrate to form millimeter-scale ink reservoirs. An AFM tip controlled by a motor touches the top plane of the reservoir. The

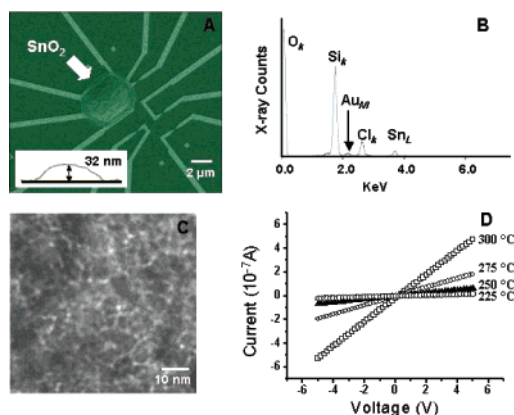


Figure 1. (A) SEM image of a miniaturized SnO_2 sensor trapped between electrodes. Inset is an AFM section profile of a deposited structure. (B) EDX spectrum collected from the sensor. (C) TEM image of a bulk SnO_2 sample after heat treatment, showing nanopores. (D) I - V curves of a SnO_2 sensor at different temperatures, showing good linearity.

amount of adsorbed ink is adjusted by varying the holding time and dip-in depth. Further adjustment can be achieved by touching the coated tip to an ink-free area on the substrate. The ink-coated tip is used to create DPN patterns on a substrate, which in the present case consists of prefabricated electrodes. Here, the cantilever does not touch the ink, which thus avoids ink-coating on laser-reflective film and makes the laser alignment easier and faster.

The sol ink is made by dissolving 1 g of block copolymer poly-(ethyleneoxide)-*block*-poly(propyleneoxide)-*block*-poly(ethyleneoxide) (P123, BASF) and 0.01 mol of tin chloride in 10 g of ethanol. Ethanol-soluble salts of titanium, cobalt, nickel, copper, zinc, cadmium, and platinum are added separately to tin chloride sol to prepare a series of inks with molar ratios to tin of 0.05. The as-prepared sols are optically translucent, with colors dependent on the metal ions. A ThermoMicroscope AFM and silicon nitride cantilevers are used for patterning in ambient conditions with a tip-surface contact force of 0.5 nN. The electrodes (20 nm gold on top of 5 nm chromium) are prepared by photolithography and electron beam deposition on silicon (100) covered with a 600-nm oxide layer. The sensors are annealed at 320 °C in air for 5–10 h before testing. After wiring out via a chip carrier, the sensor is mounted on a home-built setup, and the transport properties are monitored by a sourcemeter at a voltage of 5 V. The volume of the chamber is 300 mL, and the flow rate of balance air is controlled at 2.5 L/min.

Figure 1A shows a scanning electron micrograph (SEM) of a SnO_2 structure deposited between electrodes by holding an ink-coated tip at the location for 30 s; the length and width are 5 and 4 μm , respectively. The heights of such-formed structures range from 10 to 50 nm at the center (see the section analysis of an AFM image, inset). The composition of the structure is confirmed by energy-dispersive X-ray (EDX), which shows the expected peaks of tin, silicon, gold, oxygen, and chloride (Figure 1B). A transmis-

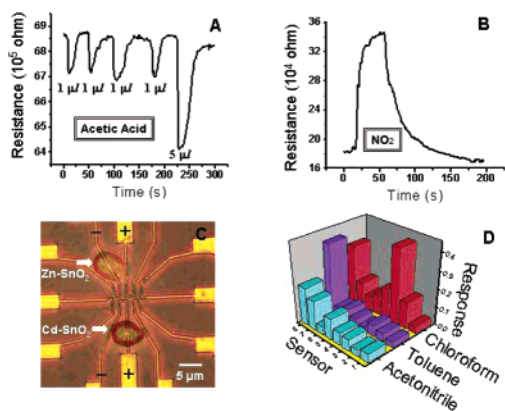


Figure 2. Sensing response of a miniaturized SnO₂ sensor to (A) acetic acid and (B) 200 ppm NO₂. (C) An optical micrograph of two sensors of an array with eight different sensors integrated on a single chip. (D) The response of each gas–sensor pair to 5- μ L exposure. The labels from 1 to 8 correspond to nominally pure SnO₂, Ti–SnO₂, Co–SnO₂, Ni–SnO₂, Cu–SnO₂, Zn–SnO₂, Cd–SnO₂, and Pt–SnO₂.

sion electron micrograph (TEM) collected on a similarly prepared bulk SnO₂ sample after heat treatment (400 °C, 2 h) in air shows the presence of nanopores (Figure 1C). The normal resistances of such tiny SnO₂ sensors at 300 °C vary from mega-ohms to hundreds of mega-ohms. The current (*I*) vs voltage (*V*) curves of one sensor are measured in pure air from 200 to 300 °C. The linear *I*–*V* curves indicate ohmic contact between the sensor and electrodes (Figure 1D).⁸

The reactions between adsorbed oxygen ions on the SnO₂ surface and reactive gases remove or add oxygen ions, influencing the conduction by releasing or trapping electrons. The performance of two miniaturized SnO₂ sensors is probed using acetic acid and nitrogen dioxide (NO₂). Injection of 1 μ L of acetic acid into the chamber at 280 °C reduces the resistance compared to that in pure air, and injection of 5 μ L leads to a larger resistance change. The sensor works repeatedly after each injection cycle (Figure 2A). A significant characteristic of the sensor is the short response and recovery time: for 1 μ L of acetic acid (equivalent concentration is 330 ppm), the resistance reaches the minimum in 5 s and recovers to its original value in 20 s. As a comparison, a conventional thin-film SnO₂ sensor shows a response time of 200 s and a recovery time of 700 s to 500 ppm acetic acid at 280 °C.^{9a} In a control experiment, we prepared a thin-film SnO₂ sensor using the same sol (thickness \sim 5 μ m and the gap between electrodes of \sim 20 μ m), where the response time and recovery time to 1 μ L of acetic acid at the same condition are 80 and 240 s, respectively. This excludes the possibility that the differences in the response and recovery times are induced by the differences in experimental conditions, such as chamber size, flow rate, and flow line. Exposure of a DPN-created sensor to NO₂ increases the resistance compared to that in air (Figure 2B). The response and recovery times to 200 ppm NO₂ at 300 °C are 20 and 65 s. This is a significantly improved performance over that of conventional Cd-doped SnO₂ sensors operated at 250 °C for the detection of 100 ppm NO₂ (50 and 480 s).^{9b} Although carbon nanotubes exhibit shorter response times (2–10 s),^{2a} longer recovery times are needed (12 h at room temperature and 1 h at 200 °C), almost like an irreversible sensor. The rapid-response and fast-recovery performance of miniaturized SnO₂ sensors is due to their small size, lower thickness, and nanoporous structure, which permit rapid diffusion of gases on to and off of active sensor surfaces.

Normal metal oxide semiconductor sensors cannot discriminate different gaseous species, and there are two methods to address this problem.¹⁰ One is to improve the sensing material to achieve

better selectivity. The other is to develop a sensor array to provide a “collective reference” for each gas. We have constructed an array with eight different sensors on a single chip that includes pure SnO₂ and its doped versions as Ti–SnO₂, Co–SnO₂, Ni–SnO₂, Cu–SnO₂, Zn–SnO₂, Cd–SnO₂, and Pt–SnO₂. Figure 2C shows an optical micrograph of two sensors of the array. The responses of each sensor to model vapors (chloroform, acetonitrile, and toluene) are studied at 300 °C by injecting 5 μ L of chemical into the chamber in the presence of airflow. The response ($R_g - R_a$)/ R_a of each gas–sensor pair, where R_a and R_g are the resistances before and after introduction of vapor, is plotted against the type of additive. For a given vapor species, the response is not the same due to the different reactivity of the gases with the sensor (Figure 2D): Pt–SnO₂ shows the largest response to acetonitrile and toluene, whereas Co–SnO₂ is more sensitive to chloroform. The resistance of all sensors is reduced when the sensor is exposed to chloroform and is increased when the sensor is exposed to acetonitrile. Collectively, such diversity in responses constitutes a reference spectrum of the miniaturized sensor array. An unknown gas can then be identified by comparing its response pattern to the reference spectrum on the array.¹¹

The sensor array with eight miniaturized sensors is the first step toward an elaborate construction of a multitude of sensors for the on-site and real-time detection of hazardous gas species. It is possible to improve sensor sensitivity by using high-melting-point metals as electrodes that enable high annealing and working temperatures, or optimizing sensor composition.

Acknowledgment. We are grateful to AFOSR-MURI, NSF-NSEC, and DOE-BES at Northwestern University for support, and Z. Zhang and Prof. V. Chandrasekhar for their assistance in wire bonding.

References

- (1) (a) Wohltjen, H.; Snow, A. W. *Anal. Chem.* **1998**, *70*, 2856. (b) Innocenzi, P.; Martucci, A.; Guglielmi, M.; Bearzotti, A.; Traversa, E. *Sens. Actuators B* **2001**, *76*, 299. (c) Domansky, K.; Liu, J.; Wang, L.-Q.; Engelhard, M. H.; Baskaran, S. *J. Mater. Res.* **2001**, *16*, 2810. (d) Zhang, G.; Liu, M. *Sens. Actuators B* **2000**, *69*, 144.
- (2) (a) Kong, J.; Franklin, N. R.; Zhou, C. W.; Chapline, M. G.; Peng, S.; Cho, K. J.; Dai, H. J. *Science* **2000**, *287*, 622. (b) Cui, Y.; Wei, Q.; Park, H.; Lieber, C. M. *Science* **2001**, *293*, 1289. (c) Law, M.; Kind, H.; Messer, B.; Kim, F.; Yang, P. D. *Angew. Chem., Int. Ed.* **2002**, *41*, 2405.
- (3) (a) Hertel, T.; Martel, R.; Avouris, P. *J. Phys. Chem. B* **1998**, *102*, 910. (b) Kwan, S.; Kim, F.; Arkan, J.; Yang, P. *J. Am. Chem. Soc.* **2001**, *123*, 4386. (c) Huang, Y.; Duan, X.; Wei, Q.; Lieber, C. M. *Science* **2001**, *291*, 630.
- (4) (a) Xia, Y. N.; Rogers, J. A.; Paul, K. E.; Whitesides, G. M. *Chem. Rev.* **1999**, *99*, 1823. (b) Heule, M.; Gauckler, L. J. *Adv. Mater.* **2001**, *13*, 1790.
- (5) (a) Pine, R.; Zhu, J.; Xu, F.; Hong, S.; Mirkin, C. A. *Science* **1999**, *283*, 661. (b) Li, Y.; Maynor, B.; Liu, J. *J. Am. Chem. Soc.* **2001**, *123*, 2105. (c) Maynor, B. W.; Filocamo, S. F.; Grinstaff, M. W.; Liu, J. *J. Am. Chem. Soc.* **2002**, *124*, 522. (d) Hong, S.; Zhu, J.; Mirkin, C. A. *Science* **1999**, *286*, 523.
- (6) Su, M.; Liu, X.; Li, S.; Dravid, V. P.; Mirkin, C. A. *J. Am. Chem. Soc.* **2002**, *124*, 1560.
- (7) (a) Fan, H.; Lu, Y.; Stump, A.; Reed, S.; Baer, T.; Schunk, S.; Perez-Luma, V.; Lopez, G.; Brinker, J. *Nature* **2000**, *405*, 56. (b) Innocenzi, P.; Martucci, A.; Guglielmi, M.; Bearzotti, A.; Traversa, E. *Sens. Actuators B* **2001**, *76*, 299.
- (8) Given SnO₂ is an n-type semiconductor and gold has a high work function, one would expect a non-ohmic contact: Kulwichi, B. M. *J. Phys. Chem. Solids* **1984**, *45*, 1015. An explanation is that the measurements here are made at high temperatures and the contact is ohmic at this voltage range.
- (9) (a) Cobianu, C.; Savaniu, C.; Siciliano, P.; Capone, S.; Urtiainen, M.; Niinisto, L. *Sens. Actuators B* **2001**, *77*, 496. (b) Sberveglieri, G.; Groppelli, S.; Nelli, P. *Sens. Actuators B* **1991**, *4*, 457.
- (10) Watson, J.; Ihokura, K. *MRS Bull.* **1999**, June 14.
- (11) (a) Lavigne, J.; Savoy, S.; Clevenger, M. B.; Ritchie, J. E.; McDaniel, B.; Yoo, S.-J.; Anslin, E. V.; McDevitt, J. T.; Shear, J. B.; Neikirk, D. *J. Am. Chem. Soc.* **1998**, *120*, 6429. (b) Albert, K. J.; Lewis, N. S.; Schauer, C. L.; Sotzing, G. A.; Stitzel, S. E.; Vaid, T. P.; Walt, D. R. *Chem. Rev.* **2000**, *100*, 2595. (c) Hagleitner, C.; Hierlemann, A.; Lange, D.; Kummer, A.; Kerness, N.; Brand, O.; Baltés, H. *Nature* **2001**, *414*, 293.

JA035727C